Host–Guest Chemistry of the Chromium-Wheel Complex $[Cr_8F_8(tBuCO_2)_{16}]$: Prediction of Inclusion Capabilities by Using an Electrostatic Potential Distribution Determined by Modeling Synchrotron X-ray Structure Factors at 16 K

Jacob Overgaard,[a] Bo B. Iversen,*[a] Sergiu P. Palii,[b, c] Grigore A. Timco,[b] Nicolae V. Gerbeleu,[b] and Finn K. Larsen*[a]

Abstract: The structure and detailed electron density distribution (EDD) of the large octanuclear chromium-wheel host complex $[Cr_8F_8(tBuCO_2)_{16}]$ (**1**) has been determined from synchrotron X-ray structure factors collected at 16(5) K. The complex has a central cavity with a minimum entry distance between carbon atoms of the pivalate methyl groups (pivalic acid = $tBuCO_2H$) of 4.027(4) Å on one side of the molecule and 7.273(4) Å on the other. The screened side of the molecule can be "opened" by rotation of methyl groups to create a strained host structure, which is compensated for by improved host–guest and host–solvent interaction. The EDD of the 272-atom complex (1144 e^-) was determined by multipole modeling based on the experimental structure factors. 3d orbital populations on the Cr atoms and topological analysis of the EDD show that the covalent part of the metal–ligand interactions consists mainly of σ donation from the ligands, but that overall the interactions are predominantly electrostatic. The electrostatic potential (EP) has been calculated from the experimental EDD. Knowledge of the geometry of the naked complex **1** as well as the EP in the central cavity of this molecule allows us to deduce which characteristic properties guest molecules must have to be accepted into the void. To probe these predictions, a series of complexes of **1** with different guest inclusions were synthesized (**2** = **1** + *N*,*N*′-dimethylformamide (DMF), **3** = **1** + *N*,*N*′-dimethylacetamide (DMA), **4** = **1** + DMA + DMF, **5** = **1** + $2CH_3CN$), and their structures were examined by using X-ray diffraction data measured at 120(1) K. Results of these studies indicate that in the crystalline state, the optimal guest molecule should be linear and possess a permanent dipole. Attempts to crystallize the host complex with cations incorporated into the cavity were fruitless, although electrospray ionization mass spectrometry showed that a [**1** + potassium]$^+$ entity pre-exists in solution and can be transferred intact into the gas phase.

Keywords: charge density · chromium · electrostatic potential · host–guest systems · supramolecular chemistry

Introduction

Host–guest chemistry has been an active area of research for many years. The first host molecule was identified more than a century ago by Villiers,[1] who discovered what later was to be known as α-cyclodextrin (α-CD). This discovery was the beginning of a search for industrially applicable CDs—a search that has recently been covered in a review by Szejtli.[2] The exploding interest in CDs and the discovery of the crown ethers[3] in 1967 resulted in the subsequent discovery of other types of compounds capable of forming supramolecular species such as cryptands,[4] cavitands,[5] carcerands,[6] calixarenes,[7] cyclophanes,[8] and many others[9] with properties similar to the CDs.[10] So far the vast majority of inclusion compounds have involved macrocyclic organic hosts,[11] whereas the discovery of new inorganic compounds displaying host-molecule properties is more recent.[12] In contrast to the

[a] Prof. B. B. Iversen, Prof. F. K. Larsen, Dr. J. Overgaard
Department of Chemistry, University of Aarhus
8000 Aarhus C (Denmark)
Fax: (+45) 8619-6199
E-mail: bo@chem.au.dk, kre@chem.au.dk

[b] Dr. S. P. Palii, Dr. G. A. Timco, Prof. N. V. Gerbeleu
Institute of Chemistry, Academy of Sciences of the Republic of Moldova, 2028 Chisinau (Moldova)

[c] Dr. S. P. Palii
Department of Chemistry, University of Florida
P.O. Box 117200, Gainesville, FL 32611-7200 (USA)

Supporting information for this article is available on the WWW under http://wiley-vch.de/home/chemistry/ or from the author. A complete list of multipolar parameters for **1** and a selection of graphical plots of the electrostatic potential are available.

  0947-6539/02/0812-2775 $ 17.50+.50/0

very organized and well-understood aqueous organic supramolecular chemistry, continuing studies of inorganic host–guest chemistry are still somewhat random. The properties displayed by the host molecule (organic or inorganic) at the binding site(s) for the guest molecules are controlled by the accessibility and the shape and size of the cavity, as well as its electrostatic environment. Determination of the geometry of the host structure has so far been obtained from X-ray crystallographic investigations,[12] whereas the (electrostatic) interactions between host and guest molecules have been estimated mainly from speculations based on the known polarity of involved functional groups or from theoretical calculations.[13] Herein we attempt to use the electrostatic potential (EP) of the undistorted (naked), ring-shaped host molecule $[Cr_8F_8(t\mathrm{BuCO_2})_{16}]$ (Figure 1) to predict properties conducive for acceptance of guest molecules. The EP is estimated from multipole modeling of extensive very low temperature synchrotron X-ray diffraction data. The predictions are tested through synthesis and structural analysis of a series of inclusion complexes with **1** acting as host (**2** = **1** + *N*,*N*′-dimethylformamide (DMF), **3** = **1** + *N*,*N*′-dimethylacetamide (DMA), **4** = **1** + DMA + DMF, **5** = **1** + $2\,CH_3CN$). Crystallographic data for the compounds investigated are summarized in Table 1. The $[Cr_8F_8(t\mathrm{BuCO_2})_{16}]$ molecule was first reported by Gerbeleu et al.[14] The magnetic anisotropy of this antiferromagnetic ring molecule was recently examined by van Slageren et al.,[15] who determined it to have the exchange parameter $J = 12\ cm^{-1}$. The hydroxo analogue of the molecule with phenylacetate bridges $[Cr_8(OH)_8(O_2CPh)_{16}]$ has been synthesized and reported by Atkinson et al.[16b] Its susceptibility data could also be modeled with one exchange parameter, $J = 12\ cm^{-1}$. Eshel et al.[16a] have synthesized a Cr_8 ring molecule with Cr atoms bridged by hydroxo and acetato ligands $[Cr_8(OH)_{12}(OAc)_{12}]$ and have examined its magnetic properties. Currently there is much interest in designing high-

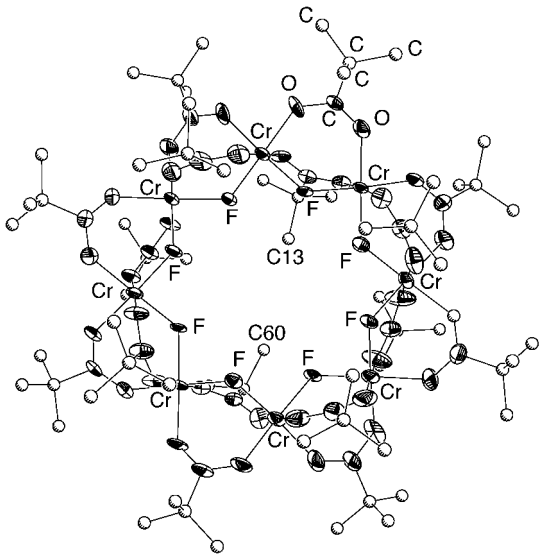

Figure 1. ORTEP drawing of **1** viewed along the normal to the chromium-wheel molecular plane. Ellipsoids truncated at 50% probability level. Positions of all Cr and F atoms of the $[Cr_8F_8Piv_{16}]$ molecule are indicated as are C and O atoms of one of the sixteen coordinating pivalate groups.

Table 1. Crystallographic and refinement details of **1**–**5**.

	1	**2**	**3**	**4**	**5**
formula: host	$Cr_8F_8C_{80}O_{32}H_{144}$	**1**	**1**	**1**	**1**·
guest inclusion	none	$[C_3H_7NO]$	$[C_4H_9NO]$	$[C_3H_7NO]\cdot[C_4H_9NO]$	$2[C_2H_3N]$
solvent of crystallization	none	none	$[C_4H_9NO]$	$4[C_4H_{10}O]$	$[C_4H_8O]$
space group	*C*2/*c*	*C*2/*c*	*Cc*	$P2_1/c$	*P*4
a [Å]	44.797(9)	45.189(5)	13.582(1)	16.241(2)	19.917(2)
b [Å]	16.468(2)	16.524(2)	29.690(1)	29.671(4)	19.917(2)
c [Å]	34.791(8)	34.703(4)	30.681(1)	29.921(4)	16.048(2)
α [°]	90.00	90	90	90	90
β [°]	115.125(2)	114.02(1)	100.71(1)	95.37(1)	90
γ [°]	90.00	90	90	90	90
V [Å^3]	23327(9)	23669(7)	12156(1)	14355(5)	6366(2)
Z	8	8	4	4	2
T [K]	16(5)	120(1)	120(1)	120(1)	120(1)
Crystal size [mm^3]	$0.1\times0.1\times0.1$	$0.4\times0.3\times0.2$	$0.3\times0.3\times0.15$	$0.4\times0.25\times0.2$	$0.4\times0.4\times0.15$
ρ_{calcd} [g cm^{-3}]	1.250	1.238	1.287	1.024	1.203
μ [mm^{-1}]	0.80	0.78	0.77	0.64	0.73
λ [Å]	0.643	0.7107	0.7107	0.7107	0.7107
N_{meas},N_{unique}	165624, 37733	139865, 35735	123157, 40484	132176, 35555	39756, 14887
$(\sin(\theta)/\lambda)_{max}$ [Å^{-1}]	0.912	0.75	0.75	0.74	0.70
R_F; R_{wF}	0.039; 0.037				
$R_F(F>4\sigma)$		0.071	0.051	0.086	0.097
R_{wF^2}	0.073	0.188	0.137	0.216	0.275
N_o/N_v	27440/1183	10614/980	26012/1030	21159/1133	14882/402
S	0.951	0.70	0.97	1.02	1.07
weighting scheme	$[\sigma^2(F_o^2)]^{-1}$	$[\sigma^2(F_o^2)+(0.078P)^2+167.21P]^{-1}$	$[\sigma^2(F_o^2)+(0.087P)^2]^{-1}$	$[\sigma^2(F_o^2)+(0.072P)^2+74.96P]^{-1}$	$[\sigma^2(F_o^2)+(0.116P)^2+30.52P]^{-1}$
VPH (= *V*/*Z*), Å^3	2916	2959	3039	3589	3183
composition of mother liquor	**1**, $C_{10}H_{21}Br$	**1**, DMF, K^+, PF_6^-, *t*BuOH	**1**, DMA, NH_4^+, PF_6^-	**1**, DMA, DMF, *t*BuOH	**1**, CH_3CN, THF, $KO_2CC(CH_3)_3$

0947-6539/02/0812-2776 $ 17.50+.50/0 *Chem. Eur. J.* **2002**, *8*, No. 12

spin cluster molecules with the aim of synthesizing single-molecule magnets, materials that may be used for storage and quantum computing. Cr_8 ring molecules being antiferromagnetic even-membered rings are characterized by an $S=0$ ground state and thus have no direct potential for use as single-molecule magnets. However, they are molecules that can be used as a starting point for further molecular engineering.

Results and Discussion

Structural details: The large number of identical bonds in a "chromium-wheel" molecule may be used to make a statistical evaluation of the molecular geometry. Selected bond lengths, averaged over similar bond lengths in **1**–**5**, are listed in Table 2. Typical standard uncertainties, as calculated from the covariance matrix of the least squares analysis for bond lengths in the individual complexes are 0.002 Å. This is lower than the standard uncertainties of the averaged bond lengths calculated from the variance of the populations. This shows that the differences among bonds of a given type are significant. These differences are currently being analyzed and they may be important in terms of fine structural correlation features, but such analysis is beyond the scope of the present study. The average Cr–$O_{carboxylate}$ bond length ($<d_{Cr-O}>$) of 1.960(6) Å appears shorter than the average value reported for a chromium-wheel,[16a] in which all fluorine atoms and every fourth carboxylate group have been replaced with hydroxo groups ($<d_{Cr-O}>=1.995(21)$ Å). No distinction can be made in **1** between the bond distances of the Cr–O bonds *trans* or *cis* to the Cr–F bonds. The observed $<d_{Cr-O}>$ in **1** is closer to the values found in two more related compounds having values of 1.968(19)[16b] and 1.947(8) Å[14]. The former is an octanuclear Cr wheel with hydroxo instead of fluorine bridges, the latter value is for a structure, where **1** acts as a host molecule with acetone inclusion. In **2**–**5**, all bond lengths for the host molecule strongly resemble the value obtained for the empty host (**1**) (Table 2). The average C–O distance of 1.259(6) Å corresponds to the C–O bond length in a completely delocalized carboxylate group ($d_{C-O}=$ 1.254(10) Å).[17] The small spread of the values furthermore illustrates that this applies to all pivalate groups. The Cr–Cr distances in **1** are on average 3.34(14) Å, which is at the high end of the range of Cr–Cr separations found in a database search of multinuclear fluorine-bridged Cr compounds.[18] This indicates that limited Cr^{III}–Cr^{III} interaction is present in **1**.

Table 2. Averaged bond lengths [Å] for **1**–**5**.

	1	**2**	**3**	**4**	**5**
$<$Cr–F$>$	1.916(6)	1.917(9)	1.917(8)	1.914(6)	1.924(5)
$<$Cr–O$>$	1.960(6)	1.955(11)	1.948(8)	1.959(9)	1.960(7)
$<$C–C$^{\alpha}>$	1.521(5)	1.523(9)	1.525(8)	1.527(8)	1.533(18)
$<$C–O$>$	1.259(6)	1.259(10)	1.260(8)	1.262(6)	1.259(15)
$<$C$^{\alpha}$–C$^{\beta}>$	1.530(10)	1.518(8)	1.523(10)	1.528(5)	1.510(30)

The structural features of the molecular host cavity and its accessibility can be specified by the smallest internuclear distance between atoms on opposite sides of the ring (Figure 1). In the center, the cavity size is controlled by distances between opposite fluorine atoms; the smallest distance between two opposite atoms is 6.470(3) Å (F3–F7). The size of the entrance to the cavity is determined by the orientation of the Me groups. On one side of the molecule, the shortest distance between carbon atoms of opposite Me groups in **1** is 4.027(4) Å (C13–C60), on the other side it is 7.273(4) Å (C25–C69). This means that the entrance to the cavity is essentially blocked on one side, whereas the other side is open to acceptance of small molecules.

This asymmetric orientation of Me groups on opposite sides of the Cr_8 ring is maintained in **2**, where the included DMF molecule is positioned slightly above the center of the cavity (Figure 2). Only a slight twist of the host molecule has decreased the closest distance between Me groups on the "closed" side to 3.95 Å and increased the closest distance on the "open" side to 7.45 Å. The DMF molecule is positioned such that the N–Me bond *trans* to the C=O bond is buried within the cavity of the host molecule. The C=O bond in DMF is parallel to the (noncrystallographic) rotation axis of the Cr wheel and points out of the host. The Me group closest to the center is displaced only 0.67 Å above the Cr_8 plane, and only 0.16 Å above the plane spanned by the four F atoms closest to DMF. This means that the DMF is exploiting the stabilization energy afforded by the nucleophilic cavity.

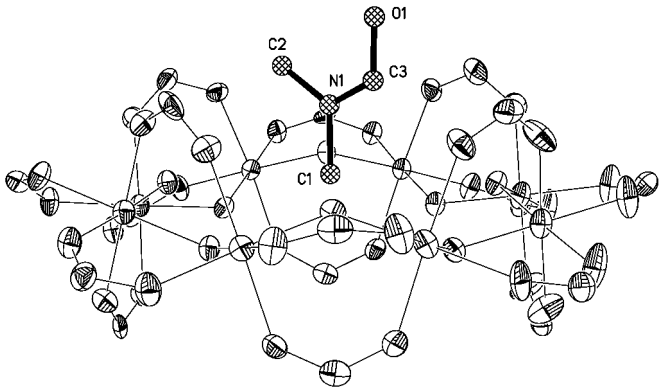

Figure 2. ORTEP drawing showing the position of DMF inside the cavity of the chromium wheel in the complex **2**. The chromium-wheel molecular plane is viewed side-on and the *t*Bu parts of the sixteen coordinating pivalate groups have been omitted from the drawing to expose better the position of the guest molecule.

In **3**, one molecule of DMA is incorporated partly into the cavity of the host molecule (Figure 3), and another DMA molecule is solvating the crystal structure. The solvation affects the packing arrangement (see below). The larger size of DMA compared with DMF prevents it from moving as deeply into the host. Furthermore, the extra Me group in DMA relative to DMF causes DMA to be differently oriented than DMF. The N–C(sp^2) bond in DMA is almost colinear with the rotation axis of the host, placing the $N(Me)_2$ end towards the center of the cavity. The innermost Me group in DMA is 2.46 Å above the Cr_8 plane, much further out than for DMF (0.67 Å in **2**). As for DMF in **2**, the inclusion of DMA in **3** has a very limited effect on the host molecule. On the

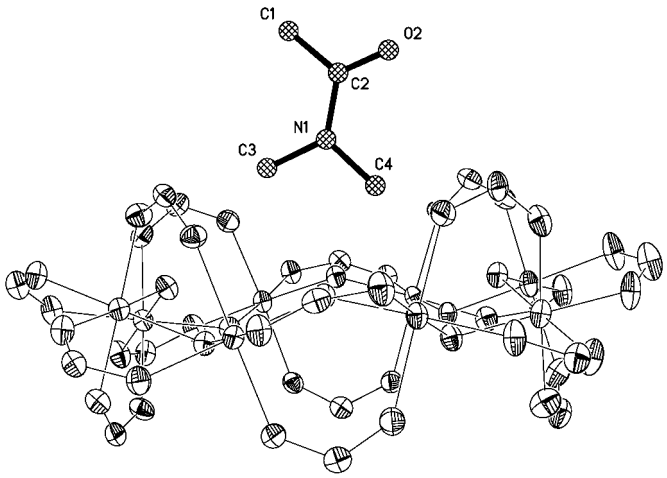

Figure 3. ORTEP drawing showing the position of DMA inside the cavity of the chromium wheel in the complex **3** presented similarly as for complex **2** in Figure 2.

"closed" side of the ring, the closest Me groups have C atoms separated by 4.12 Å, slightly more than for **1**, whereas on the "open" side the smallest separation has increased to 7.90 Å.

Surprisingly, **4** exhibits guest molecules both above (DMA) and below (DMF) the center of the host (Figure 4). The

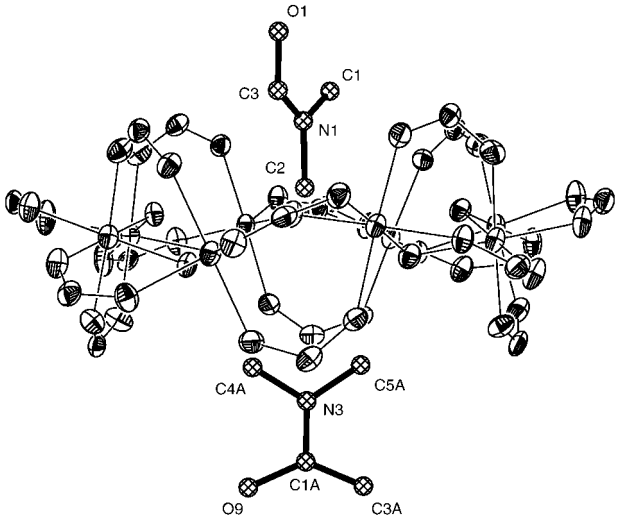

Figure 4. ORTEP drawing showing the position of DMF and DMA inside the cavity of the chromium wheel in the complex **4** presented similarly as for complex **2** in Figure 2.

methyl group of DMA closest to the host molecule center is placed 2.83 Å above the Cr_8-plane on the open side and the methyl group of DMF is 1.03 Å below this plane on the closed side. To accomodate both these molecules, the host molecule is altered significantly. The closed side has been opened to achieve a smallest cross-opening C^β–C^β separation of 6.965(5) Å—an increase of almost 3.0 Å compared to that in **1**. This cannot be accomplished exclusively by the rotation of Me groups, and must be accompanied by an increased strain in the ring. The C^α–C^α distances are well-suited to quantify the internal molecular strain of the host molecule as they are independent of the orientations of the Me groups. Examination of C^α–C^α distances (Table 3) shows that the inclusion of either DMF or DMA (**2** or **3**) through the open side only affects the host molecule very little and mainly by rotation of Me groups with a concomitant increase in C^β–C^β separations. Inclusion on both sides (**4**) of the host leads to a large increase in C^α–C^α distance (from 7 to 8.9 Å) on the originally closed side, and the entrances in **4** have become very similar, which implies that the host has been significantly twisted. Crystals of complex **4** contains four *t*BuOH molecules of crystallization in the structure. One of these solvent molecules forms a rather short hydrogen bond with the DMA guest molecule (d_{O-O} = 2.64 Å), while no significant hydrogen bonds are formed between the solvent and the host molecule or DMF, showing that the effect of solvation on the opening of the closed side for inclusion is indirect.

Table 3. Cross-opening distances [Å] that determine the entrance sizes to the cavity. Owing to the crystallographic fourfold axis the maximum and minimum distances are identical for compound **5**.

Bonds	**1**	**2**	**3**	**4**	**5A**	**5B**
open side						
$d(C^\alpha–C^\alpha)_{min}$	9.413(4)	9.182(5)	9.198(5)	9.126(5)	9.183(6)	9.063(7)
$d(C^\alpha–C^\alpha)_{max}$	9.519(4)	10.343(4)	10.437(5)	10.354(5)		
$d(C^\beta–C^\beta)_{min}$	7.274(4)	7.458(5)	7.982(5)	7.793(5)	7.242(6)	7.341(7)
$d(C^\beta–C^\beta)_{max}$	7.524(4)	8.773(5)	9.463(5)	9.342(5)		
closed side						
$d(C^\alpha–C^\alpha)_{min}$	7.028(4)	6.932(5)	6.941(5)	8.907(5)	9.061(6)	8.238(6)
$d(C^\alpha–C^\alpha)_{max}$	9.217(4)	9.366(5)	9.785(5)	10.483(5)		
$d(C^\beta–C^\beta)_{min}$	4.023(4)	3.971(5)	4.207(4)	6.965(5)	7.204(6)	5.646(7)
$d(C^\beta–C^\beta)_{max}$	7.033(4)	7.037(5)	7.332(5)	9.092(5)		

Compound **5** is significantly different from the previous complexes. There are two crystallographically independent host molecules in **5** (A and B), which exhibit slightly different orientation of Me groups (Table 3). The aromatic solvent molecules (THF) are positioned exactly between the host molecules and are disordered. Acetonitrile molecules have entered the cavity from both sides (Figure 5). The guest molecules have deeply entered the cavity, with the Me end closest to the center. The methyl carbon atom closest to the center, C99, is only 0.56 Å above the Cr_8 plane.

Packing patterns: Figure 6 shows packing diagrams for compounds **1**–**5**. Only one packing plot for **1** and **2** is shown in Figure 6, since they crystallize in identical patterns. Compounds **1**–**4** exhibit quite similar packing patterns, which are reminiscent of honeycomb-packed stacks of tilted host molecules. The main difference between **1**–**4** is the inclination angle between adjacent Cr_8 rings (**1** and **2**, 33.8°; **3**, 14.4°; **4**, 89.2°). In **4**, the large amount of solvent has significantly increased the unit cell volume and the relative orientations of the Cr_8 rings, but the basic packing of the hosts remains unchanged. The packing in the tetragonal space group (**5**) is fundamentally different from **1**–**4**. Every Cr_8 ring is surrounded by four Cr_8 rings, each of the latter are parallel to and in the same plane as the first Cr_8 ring. Judging from the cell volume this packing seems to be as tight as for **1**–**4**. It is interesting to note that complete inclusion of a guest molecule (such as in **2**) has very little effect on the outer envelope of the molecule. This is seen by the fact that compounds **1** and **2** have virtually identical crystal packing and cell volume, that is, the electrostatic envelope of the molecule is unaffected by its interior.

  0947-6539/02/0812-2778 $ 17.50+.50/0 *Chem. Eur. J.* **2002**, *8*, No. 12

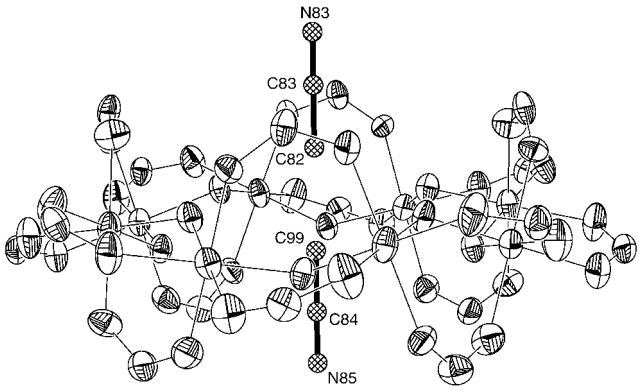

Figure 5. ORTEP drawing showing the position of CH_3CN inside the cavity of the chromium wheel in the complex **5** presented similarly as for complex **2** in Figure 2.

The electron density in compound 1: The refined values of the monopoles can be used to estimate atomic charges. The average charge for Cr is $+0.55(5)$ e, much below the nominal charge of $+3$, reflecting the significant electron donation from the ligands. Low metal atomic charges have also been observed in other electron density studies of Cr complexes.[19] For F and O, the net average atomic charges are $-0.53(4)$ and $-0.36(3)$, respectively. Both C and C^{α} atoms are negatively charged due to the electron-withdrawing oxygen atoms ($-0.25(5)$ e and $-0.22(4)$ e, respectively). The

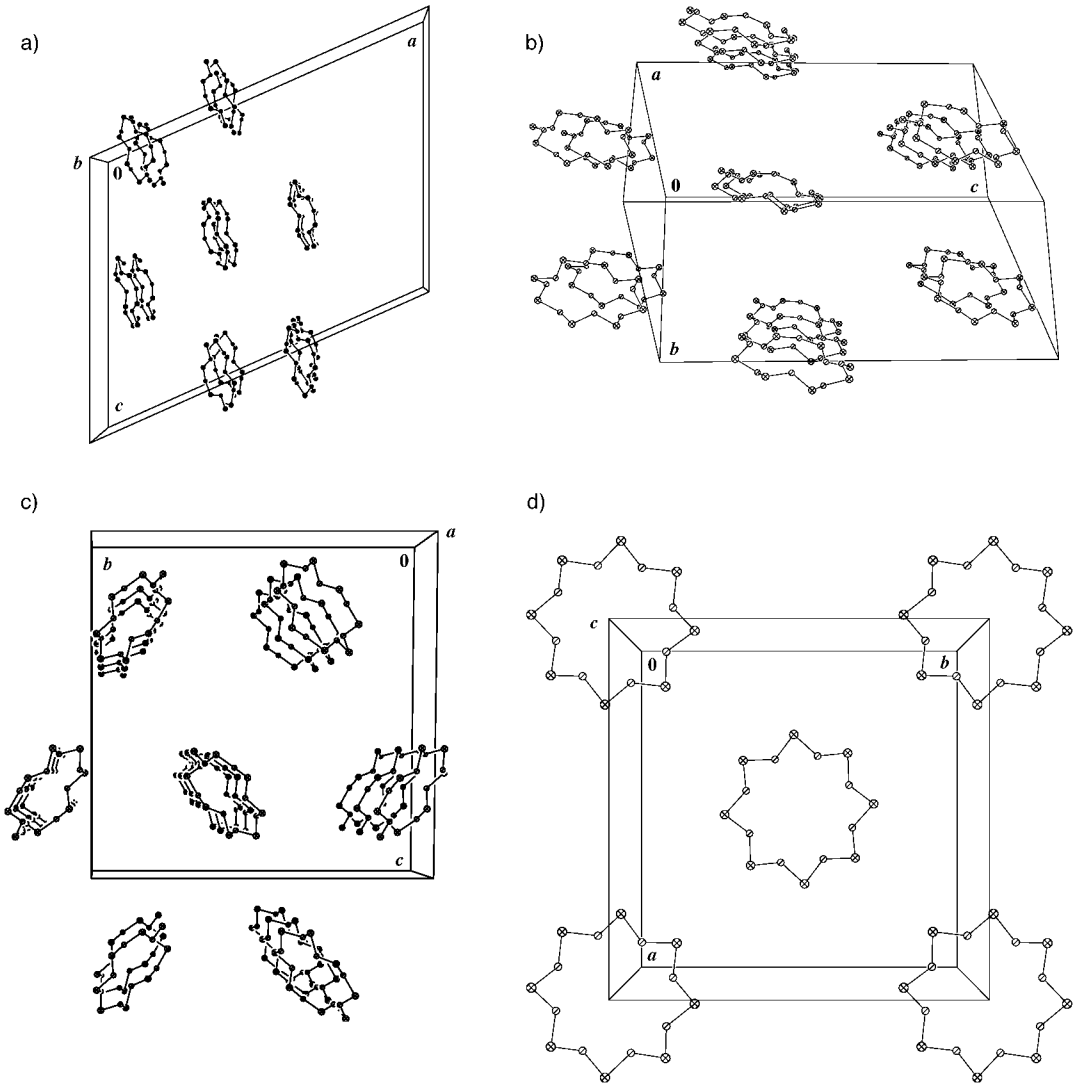

Figure 6. Packing diagrams for a) **1**, b) **3**, c) **4**, and d) **5**. For clarity only Cr and F atoms of the chromium wheels are shown.

Me groups carry an average net positive charge of +0.39(1) e. Similar charge distributions in pivalate groups have been observed in other studies.[20]

Figure 7 depicts two model deformation density (DD) maps. The lone pair regions near the ligands in the Cr–O bonds and in the Cr–F bonds are very significant. Excess

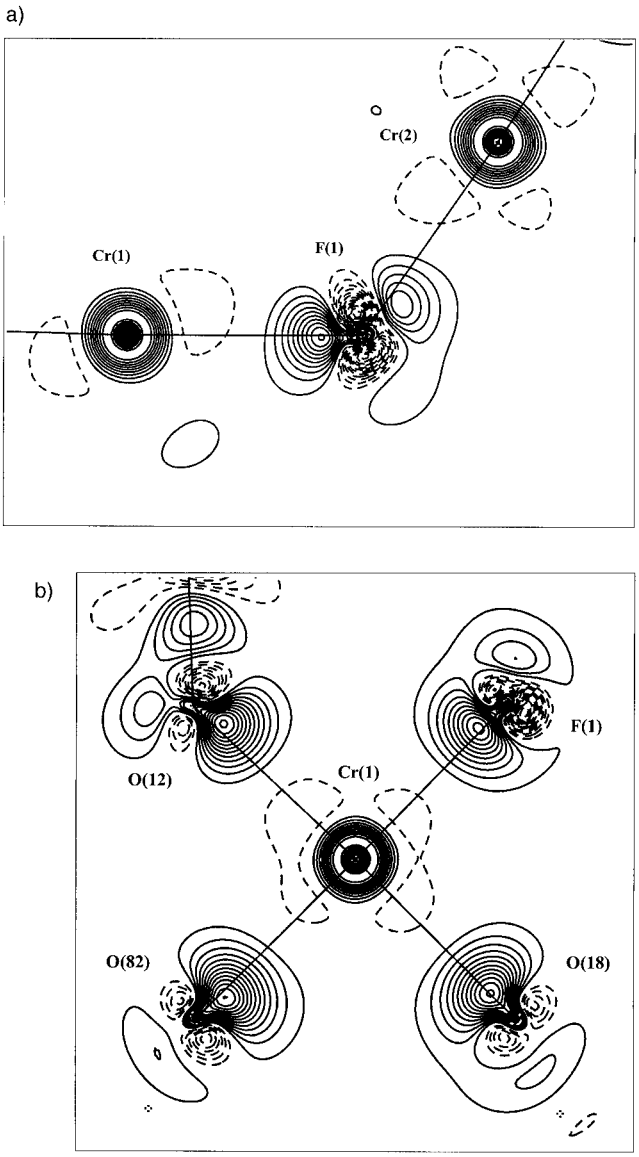

Figure 7. Deformation density maps of Cr–F and Cr–O bonds represented by a) the Cr(1)-F(1)-Cr(2) plane, and b) the F(1)-O(18)-Cr(1)-O(12)-O(82) plane. Solid lines are positive contours, negative contours are dashed. Zero contour is omitted.

density in the bonding directions is expected if the modeling of the EDD has been successful. The DD around Cr is almost completely spherical, with only one negative contour in the bonding directions breaking significantly the spherical symmetry. The model bonding density can also be visualized by plotting the Laplacian of the density in the same planes (Figure 8). The positive peaks correspond to charge concentration (bonding density), and the negative peaks to charge

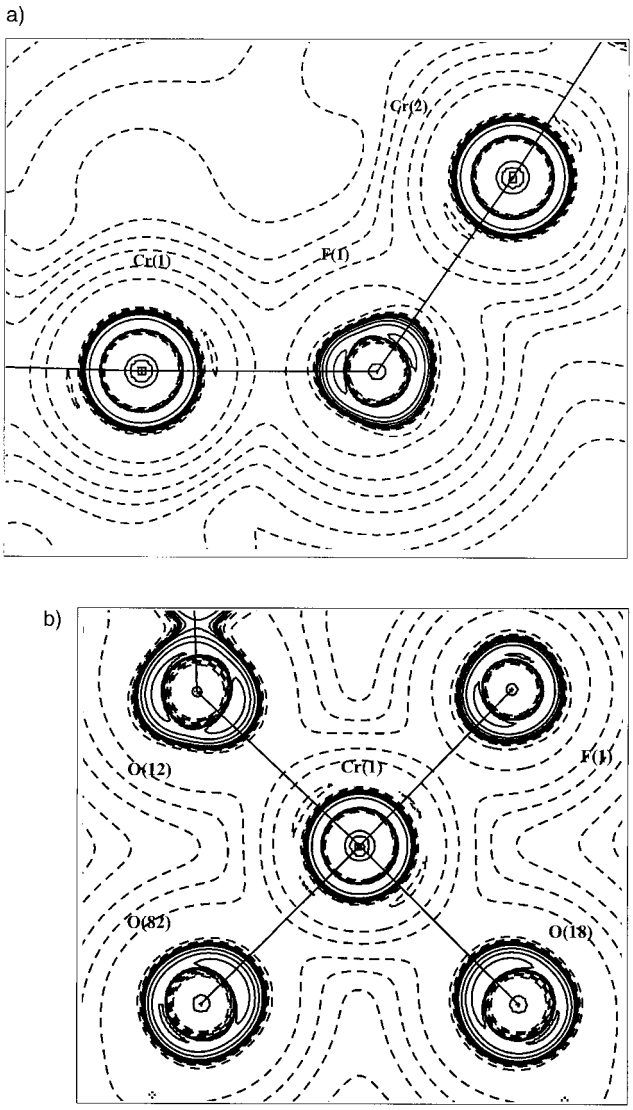

Figure 8. Laplacian plots of the planes shown in Figure 7. Contours at 2, 4, and 8×10^n, $n = -3, -2, -1,0,1,2$.

depletion. These plots confirm the lone pair features on the ligands to Cr and the lack of asphericity on Cr.

We have performed a topological analysis of the total static electron density within the framework of the "quantum theory of atoms in molecules".[21] Table 4 lists average values of topological properties like the density (ρ_b) and the Laplacian ($\nabla^2\rho_b$) at the bond critical points (bcp). The esds (sample standard deviations) for the topological properties to some extent reflect the slight differences in bond lengths among similar bonds. It is illustrative to examine in more detail the Cr–ligand interactions. The energy densities at the bcp can be calculated for closed-shell interactions using the semiempirical formula given by Abramov.[22] Average values for these properties are given in Table 4. The kinetic (G) and potential (V) energy densities cancel almost exactly in both Cr–F and Cr–O bcp, such that the total energy density (H) is close to zero. The value of $G(r_{bcp})/\rho_b$ is about 1.80, showing that these bonds are closed-shell interactions.[22b] Thus, the Cr–O and Cr–F bonds are similar in character, which explains why there is no observable *trans* effect.

  0947-6539/02/0812-2780 $ 17.50+.50/0 *Chem. Eur. J.* **2002**, *8*, No. 12

Table 4. Mean values of the topological indicators and the energy densities of **1**.

Bond	ρ_b [e Å^{-3}]	$\nabla^2\rho_b$ [e Å^{-5}]	V [hartree Å^{-3}]	H [hartree Å^{-3}]	G/ρ [hartree e^{-1}]
Cr–F	0.62(2)	16.3(5)	–1.10(4)	0.02(2)	1.81(4)
Cr–O	0.58(3)	15.2(9)	–1.01(5)	0.03(5)	1.78(10)
C–O	2.95(3)	– 47.2(12)	–	–	–
C^{α}–C^{β}	1.68(1)	– 12.6(3)	–	–	–

Table 5. d-orbital populations. Values for two compounds from reference [24] are also given.

Orbital	**1**	$Cr(CN)_6^{3-}$	$Cr(CO)_6$
d_{z^2}	0.91(5)		
$d_{x^2-y^2}$	0.71(5)		
e_g	1.62(5) (29.7 %)	1.62(5) (30.8 %)	1.37(5) (29.2 %)
d_{xy}	1.51(5)		
d_{yz}	1.00(5)		
d_{xz}	1.32(5)		
t_{2g}	3.83(5) (70.3 %)	3.64(5) (69.2 %)	3.32(5) (70.8 %)
total	5.45(5)	5.26(5)	4.69(5)

Table 5 lists the extracted d-orbital populations[23] for Cr. For comparison, the values for two other octahedral Cr complexes[24] are also shown. The destabilizing e_g orbitals accept almost the same number of electrons from the σ-donating ligands, whereas the population in the t_{2g} orbitals reflect the π-accepting ability of the ligands. In this respect, CO and CN^- are superior to F^- and the O-atom of a carboxylate group.

Electrostatic potential in compound 1: The electrostatic potential in the host molecule in the crystal environment has been derived from the refined multipole parameters according to the method of Su and Coppens.[25] Figure 9

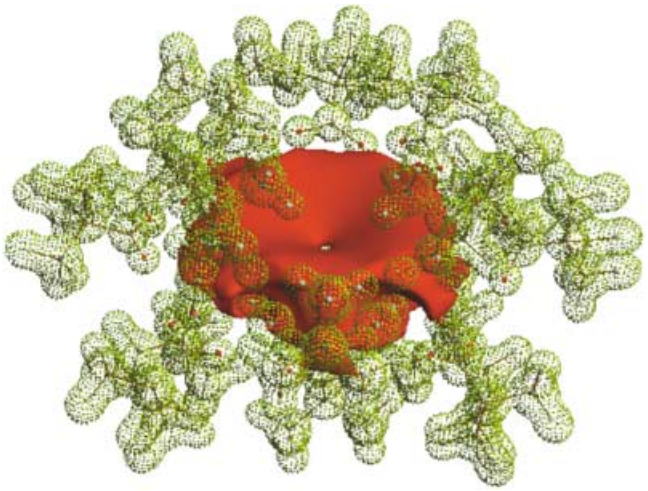

Figure 9. Isosurface plot of the electrostatic potential in **1**. Surface at -0.54 e Å^{-1} (red) and $+0.3$ e Å^{-1} (yellow).

illustrates the three-dimensional features of the EP in **1** using negative (red) and positive (yellow) isosurfaces. In Figure 9 it is seen that the isosurface outlined at the value of the EP in the center of the cavity has a funnel-shaped form. The view in Figure 9 is from the "open" side of **1**, but the shape is similar when viewed from the other side. There is a three-dimensional saddle point in the EP located at the molecular center with a minimum along the axis perpendicular to the Cr_8 plane and a maximum within this plane. The local character of the positive isosurfaces shows that the electrophilic regions are closely confined to the Me groups on the outside of the molecule. The negative region of the EP hardly protrudes out of the cavity entrance on the "open" side (Figure 10a). It extends from the sides of the molecule in regions between the axial and the equatorial pivalate ligands. The negative EP is almost exactly symmetrical with respect to the Cr_8 plane, Figure 10a. The first negative contour shown (-0.1 e Å^{-1}) extends outside the "open" side, whereas this contour is within the molecule on the opposite side. In the molecular cavity, the negative potential reaches a local minimum along the molecular axis at the center with a value of -1.24 e Å^{-1}. The central potential is quite flat and Figure 10b shows that the area of negative potential within 5 % of the center value (-1.24 e Å^{-1}) spans a circular area with a radius of more than 2 Å.

Influence of the EP on host–guest chemistry: The detailed nature of the EP in host **1**, described in the previous section, affords a qualitative explanation of the observed differences in the structures **2**–**5**. Furthermore, the knowledge of the EP allows us to predict the features required by different guest molecules to be incorporated inside **1**. From the EP it is clear that guest molecules have to be oriented quite specifically for inclusion to occur, since positive guest entities will be repelled by the outer molecular envelope, before they attain stabilization in the center. Thus, there must be a considerable barrier for inclusion. The weakness of the inclusion capabilities may be used for selectivity because only a limited number of small molecules can be bound in the crystal. An extended linear molecule with a permanent dipole will be able to stabilize both ends of the molecule by being placed asymmetrically with the positive end inside the cavity and the negative end outside the cavity. It is not favorable to place a permanent dipole totally inside the host (that is, symmetric inclusion across the molecular center). From the EP we therefore predict that neutral molecules will be bound only weakly, whereas one-dimensional molecules (chains) having a permanent dipole moment can be stabilized asymmetrically. Small positive cations can be stabilized in the molecular cavity but, as will be shown below, crystallization of such host–guest complexes have not been possible, and they only appear in the liquid and the gas phase. Negative ions may be able to associate with the outer envelope of the molecule.

The inclusion of DMF is expected to be favorable, as it exhibits two oppositely polarized ends. In one end, two Me groups are bonded to a more electronegative nitrogen, creating two electrophilic Me groups. In the other end, the oxygen is highly nucleophilic. Thus, the $N(Me)_2$-end will supposedly be closest to the nucleophilic maximum in the center of the host. To minimize repulsion between the nucleophilic oxygen and the nucleophilic cavity, the C=O bond is parallel to the molecular axis. Thus, the *trans* N–C bond is along the same axis, thereby increasing the steric

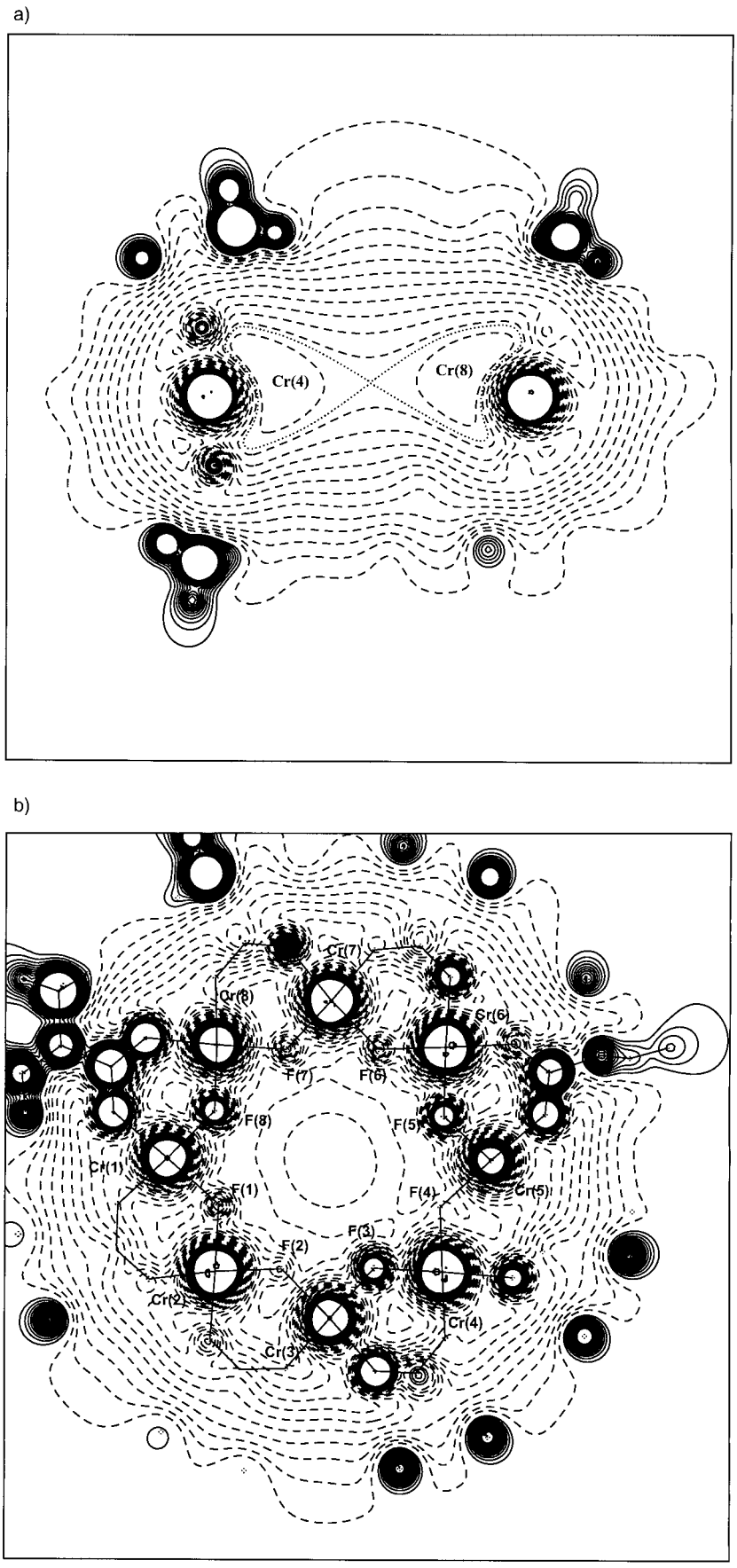

Figure 10. Contour plots of the electrostatic potential in **1**. Contour interval of 0.1 e Å^{-1}. Negative contours dashed. Positive contours solid. Zero contour omitted. a) The perpendicular plane through Cr(4) and C(8). b) The molecular plane through Cr(1), Cr(3), and Cr(4).

hindrance from the *cis*-Me group, which points towards the host. Nevertheless, it seems favorable to align the C=O bond along the molecular axis, showing the importance of the electrostatic contribution to the interaction energy.

Inclusion of the larger DMA into **1** is also favorable for the same reasons as DMF, although the larger size of DMA decreases the stabilizing effect of inclusion due to steric hindrance. The substitution of a Me for a H on the carbonyl carbon creates a larger molecule, which necessitates a rotation of DMA (compared to DMF) in order to better accomodate this extra Me group. The requirement of more space prevents DMA from being as deeply buried into the host molecule, which is reflected in the shortest distance from DMA to the plane spanned by the eight Cr atoms, having increased from 0.67 (in **2**) to 2.46 Å (in **3**).

As mentioned in the previous section, the EP is negative both towards the "open" and the "closed" sides. Steric hindrance makes the entry of guests through the "closed" side unfavorable, but a rotation of axial pivalate Me groups on this side can increase the affinity for guests to reach the cavity. This appears to be the case for **4**. Since the most energetically favorable configuration of the host exhibits one "closed" side of the ring structure (**1**), the configuration of the host must have changed due to the presence of either the included DMA or the inclusion of solvent *t*BuOH—which forms a strong hydrogen-bonding network—or both. Since DMA is the only solvent in **3**, and it does not affect the "closed" side, the *t*BuOH must play a major part in the "opening" of **1** by providing hydrogen-bonding stabilization energy.

In **5** two molecules of CH_3CN have found their way into the

  0947-6539/02/0812-2782 $ 17.50+.50/0 *Chem. Eur. J.* **2002**, *8*, No. 12

structure. The incorporation of CH_3CN into an inorganic host molecule has been observed before.[13, 26] The host in reference [26] is categorized as electronically inverse, in contrast to **1**, which is an electronically normal host. This is evident in the orientation of CH_3CN, which possesses a permanent dipole, the nitrogen end being negatively polarized. The positively polarized carbon end is near the center in **5**, whereas the opposite is the case in reference [26].

Mass spectrometry of the host–guest mother solution: The existence of a nucleophilic region in the host molecular cavity suggests that cations should be strongly attracted to this region. Attempts to crystallize the host complex with cations incorporated into the cavity were fruitless (see Table 1). The lack of cation incorporation observed in the crystalline samples may not exclude the existence of such host–guest entities in solution prior to crystallization. To test this assumption, the mother solution of sample **2** was investigated by means of electrospray ionization mass spectrometry (ESI-MS).[27] The choice of this method was determined by its "gentleness", meaning that ionic species with weak interactions such as in supramolecular assemblies, poly-solvated aggregates, host–guest entities, and noncovalent complexes, survive the transfer from solution to the gas phase and thus can be detected and identified by mass spectrometry.[28] The ESI mass spectrum shown in Figure 11 confirmed unambiguously that a cation can be associated to the host molecule **1**. Analysis of experimentally determined isotopic distributions, performed by the ISOMETA program,[30b] shows that the group of peaks seen in the m/z 2220–2230 mass region represents an isotope cluster with an elemental composition of $[\mathbf{1}+K]^+$. Furthermore, the $[\mathbf{1}+K]^+$ ion produces an insignificant yield of fragments when accelerated in the atmosphere–vacuum interface region of the ESI source by increasing capillary and/or skimmer voltages in an attempt to initiate collision-induced dissociation processes. Also, an increase in the ion accumulation time in the hexapole of the ESI source in order to create conditions for multipole storage assisted dissociation (MSAD)[28k, 29] did not lead to any significant fragmentation. These findings prove that the $[\mathbf{1}+K]^+$ species is quite stable in the gas phase, where counterions and solvation effects are absent. ESI-MS data, together with the lack of crystallographic evidence for the host–guest entity $[\mathbf{1}+\text{cation}]^+$, indicates that it exists in solution but not in the solid state.

This may be due to a destabilizing effect of the anion in the crystallization process—an effect large enough to impede the crystallization of the cation-containing host–guest complex and instead enables the crystallization only of the unsolvated species or with neutral solvent included. Since the inclusion of cation–anion pairs is so unfavorable, it may be that only neutral species can be accepted into the host in the crystalline phase. Due to steric hindrance these guests can only have limited size, and the smaller guests tend to be more strongly attached to the host, although guests may leave the solid phase if left exposed to air. Thus, the optimal guest molecule will possess a permanent dipole and have a limited range at least in two dimensions. These guidelines and the stability of **1** in some solvents may be exploited as a means for selectively extracting certain molecular entities.

Conclusion

A multipolar refinement based on accurate synchrotron X-ray data collected at 16(5) K with a new open He-cooling system has succesfully been carried out on the molecular complex, $[Cr_8F_8(t\text{BuCO}_2)_{16}]$, containing 272 unique atoms (1144 e^-), of which eight were open-shell transition metals. Theoretical calculations of accurate electron density distributions of molecules of this size are very demanding. The present study demonstrates that experimental electron density determination, including full topological analysis, can be carried out on supramolecular systems provided that crystals of reasonable quality can be obtained. It must be stressed that the restriction on the crystal has mostly to do with, for example, lack of disorder rather than crystal size, since modern synchrotron sources have made diffraction experiments possible even with crystals with dimensions in the order of micrometers. The general agreement with other studies containing similar structural entities shows that it is possible to obtain chemically useful experimental EDDs for huge systems. The fact that the EDD appears accurate suggests that the electrostatic potential is very reliable (primarily determined by the low order data). A detailed description of the electrostatic potential in the interior of the host molecule has been used to explain the

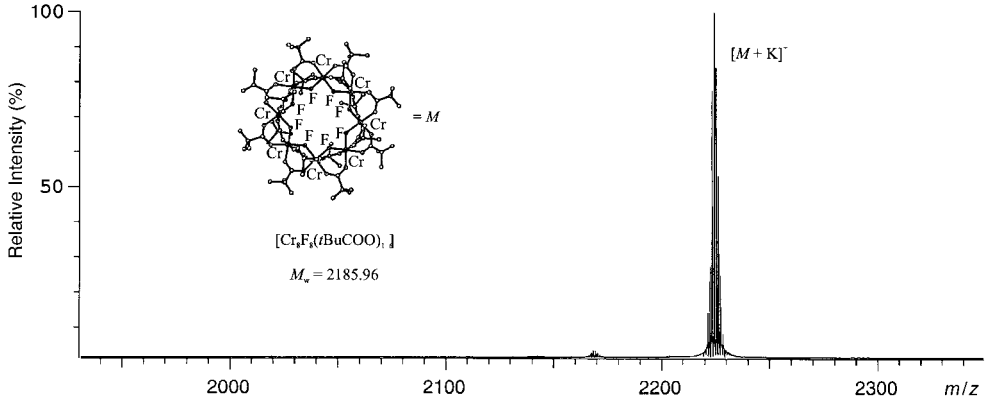

Figure 11. Positive-ion ESI mass spectrum[27] of the mother solution of sample **2** diluted (1:10) with CH_2Cl_2. Experimental parameters: capillary voltage = 50 V, skimmer voltage = 5 V, ion accumulation time in the hexapole of the ESI source = 0.5 s, capillary temperature = 110 °C.

orientation of guest molecules in a series of host–guest complexes with **1** acting as a host. Supramolecular and inclusion chemistry is a rapidly expanding field of increasing importance and it is clear that analysis of experimental electron densities presents a versatile new tool to structural chemists.

Experimental Section

Synthesis: The starting material of the octanuclear chromium-wheel compound used in the preparation of the host–guest complexes described in this paper was synthesized by modifying the method previously reported.[14]

$CrF_3 \cdot 4H_2O$ (5.0 g, 27.62 mmol), DMF (8.5 mL, 110.0 mmol), and pivalic acid (tBuCO$_2$H = PivH) (11.5 g, 112.6 mmol) were heated while stirring at 140 °C for 2 h. During this time chromium fluoride was dissolved and a green crystalline product formed. The solution was cooled to room temperature, and the following day the crystalline product was first washed with DMF (3×20 mL) until the solution was transparent, then with water (5×20 mL). Then the product was dried at 120 °C for 2 h and dissolved in pentane (40 mL). The resulting solution was filtered and then diluted by adding acetone (80 mL). This solution was refluxed with stirring for 30 min, and then concentrated to 30 mL. The resulting crystals were collected by filtration and washed with acetone. This product ($[Cr_8F_8Piv_{16}] \cdot 2Me_2CO$) was dried at 120 °C to constant mass. Acetone was thereby expelled and a powder of $[Cr_8F_8Piv_{16}]$ was obtained with no inclusion of solvent molecules. Yield 2.0 g (26.5 %); MS (EI):[30] m/z: 2084.4 $[M-\text{Piv}]^+$ (where $M = [Cr_8F_8Piv_{16}]$); elemental analysis calcd (%) for $C_{80}H_{144}Cr_8F_8O_{32}$ (2186.0): C 43.96, H 6.64, F 6.95; found: C 43.87, H 6.68, F 6.88.

Crystal growth: *Compound* ***1***: $[Cr_8F_8Piv_{16}]$ (0.5 g) was dissolved while stirring in 1-bromodecane (5 mL) at 200 °C. The solution was slowly cooled to room temperature. After one week, dark green crystals of **1**, the naked complex without guest molecules, were collected. For the host–guest complexes, compounds **2**–**5**, the main purpose of the syntheses was to obtain pure compounds and good crystals. The yield was about 50 %. No optimization of the yield was attempted and therefore it is not reported specifically for the following syntheses.

Compound ***2***: $[Cr_8F_8Piv_{16}] \cdot$ DMF. $[Cr_8F_8Piv_{16}]$ (0.3 g) and KPF_6 (0.15 g) were heated while stirring and refluxing in DMF (3.0 mL) and tBuOH (3.0 g) for 15 min. The hot solution was filtered and kept at 50–60 °C for 7 h at which time green crystals of **2** (=**1** + DMF) had formed.

Compound ***3***: $[Cr_8F_8Piv_{16}] \cdot 2$DMA. NH_4PF_6 (0.1 g) was dissolved in DMA (5.0 mL) while heating (80 °C), then $[Cr_8F_8Piv_{16}]$ (0.03 g) was added and the mixture heated until complete dissolution was observed. The resulting solution was cooled to 90–100 °C and kept at this temperature for 7 h, yielding green crystals of **3**, which have DMA molecules as guest molecules in the chromium wheel but also DMA molecules solvating the crystal structure.

Compound ***4***: $[Cr_8F_8Piv_{16}] \cdot$ DMF $\cdot$ DMA $\cdot 4t$BuOH. $[Cr_8F_8Piv_{16}]$ (0.1 g) was heated while stirring and refluxing in a mixture of tBuOH (3.0 mL), DMF (2.0 mL) and DMA (0.1 mL). The hot solution was filtered and kept at 50–60 °C for 7 h, yielding green crystals of **4**, which have DMF and DMA as guest molecules in the chromium wheel and tBuOH molecules solvating the crystal structure.

Compound ***5***: $[Cr_8F_8Piv_{16}] \cdot 2CH_3CN \cdot$ THF
$[Cr_8F_8Piv_{16}]$ (0.3 g) was dissolved in tetrahydrofuran (THF) (9.0 mL), then acetonitrile (3.0 mL) was added to a hot solution and the solution refluxed for 5 min. It was left to stand overnight at room temperature. Large green crystals of **5** were formed, which have CH_3CN as guest molecules in the chromium wheel and THF molecules solvating the crystal structure.

X-ray data collection and treatment: *Compound* ***1***: A crystal of approximately $0.10 \times 0.10 \times 0.10$ mm was attached to a few strands of carbon fibers using a very small amount of epoxy glue. The fibers were attached to a brass pin that had been glued onto a copper wire. The brass pin was mounted directly on the ϕ axis of a HUBER-type 511 four-circle diffractometer at the X3 A1 beam line at the National Synchrotron Light Source (Brookhaven National Laboratory, USA). The crystal was cooled in one hour to 16(5) K using an open-flow He-cooling device.[31] Diffraction data were collected with a Bruker SMART 1000 CCD detector placed on the 2θ-arm with the detector surface 5.7 cm from the crystal. Two different 2θ settings were used for the measurements in ϕ scan mode. Integration of the intensities was performed by using SAINT+[32] and an empirical absorption correction was applied by using SADABS.[32] A few reflections at small scattering angles, which were partly hidden by the beam stop, were discarded. Only multiple-measured reflections were retained for further analysis. The final data set, averaged with SORTAV,[33] comprises 37 733 multiple-measured unique reflections with an average redundancy of 4.4 ($R_{int} = 0.034$). Refer to Table 1 for further details.

Compounds **2**–**5**: X-ray diffraction experiments for these four systems were carried out using a Bruker SMART CCD diffractometer equipped with a Mo X-ray tube at the Department of Chemistry, University of Aarhus. In all cases the selected crystals were mounted on the tip of a glass pin using Paratone-N oil and placed in the cold flow (120 K) produced with an Oxford Cryocooling device. Complete hemispheres of data were collected using ω scans (0.3°, 30 seconds/frame). Integrated intensities were obtained with SAINT+[32] and corrected for absorption using SADABS.[32] Structure solution and refinement was performed with the SHELX package.[32] Crystallographic details are given in Table 1.

Model refinement: *Compound* ***1***: Initial refinements with SHELX,[32] which were started from the previously determined 100 K structure of **1**, yielded a structural model with $R(F) = 0.039$ for $I > 2\sigma(I)$. Potential disorder in the *tert*-butyl part of three of the pivalate groups can for each group be tested with a model consisting of two sets of sites, both with isotropically vibrating methyl groups (Model A). In an ordered description one set of fully occupied sites with anisotropically vibrating methyl groups is used (Model B). The ordered model for the three pivalates is superior when comparing refinement statistics: $R_A(F) = 0.049$, $R_B(F) = 0.039$.

The SHELX structural skeleton was the starting point for a refinement using the program package XD,[34] which incorporates the Hansen–Coppens multipole formalism[35] to describe the asphericity of the EDD around each atomic position. Neutral atom scattering factors were employed[36] and the radial part of the multipoles were of single Slater type. Due to the large size of the molecule, it was necessary to generate constraints, which could be relaxed at later stages of the modeling. In the first multipole model (MM-I) we constrained atoms of the same type to have identical population parameters. Gradual release of constraints reduced $R(F^2)$ from 0.062 for the most constrained model to 0.055 for the final model, which included 1582 parameters. In this model all atoms, except for the methyl-C atoms and the hydrogens, were given individual full sets of multipoles truncated at the hexadecapolar level ($l = 4$) for Cr and the octapolar level ($l = 3$) for the other atoms. The three methyl groups in each pivalate ligand were constrained to be identical with a common set of multipoles truncated at quadrupolar level ($l = 2$). Hydrogen atoms were given one common monopole and one common bond-directed dipole. The radial distribution of the spherical density for each non hydrogen atom type was refined using a κ' parameter. Due to correlation effects, it was necessary to refine multipole parameters and structural parameters in separate cycles.
Subsequently, we examined the significance of the noncrystallographic symmetry, inherent in the molecular structure. In this refinement (MM-II), all atoms of similar type were constrained to have identical deformation parameters. The starting point was MM-I. The monopoles were averaged and the starting values for the multipoles were taken from the first atom of each type in the atom list. The level of truncation for the multipoles was identical to MM-I. We distinguished between six different atom types: Cr, F, O, C (COO^-), C^α (CR_4), and C^β ($C{-}CH_3$). Due to the smaller number of parameters in this model, structural parameters for all heavy atoms could be co-refined with the multipoles. In the final cycles of the refinement, the hydrogen atoms were repositioned along the C–H bond vector to a distance of 1.08 Å from the bonded carbon.

To test the success of the refinement we examined in each step both the refinement statistics and several residual maps. The continuous decrease of both R values and general contour levels in the residual maps indicated that the modeling was successful, considering the size of the molecule. Figure 12 shows the residual density in the molecular plane from the final MM-II. The maximum value of -0.4 e Å^{-3} near a Cr atom is acceptable for this large molecule. The Hirshfeld rigid bond test[37] gives a mean value of $\Delta_{A\text{-}B} = 15.4$ pm^2 for all bonds, and for bonds to Cr the mean value is 9.4 pm^2 (Cr–F: 11 pm^2; Cr–O: 8.0 pm^2). The relatively large size of the atomic displacement parameters for three of the pivalate groups contribute to the

  0947-6539/02/0812-2784 $ 17.50+.50/0 *Chem. Eur. J.* **2002**, *8*, No. 12

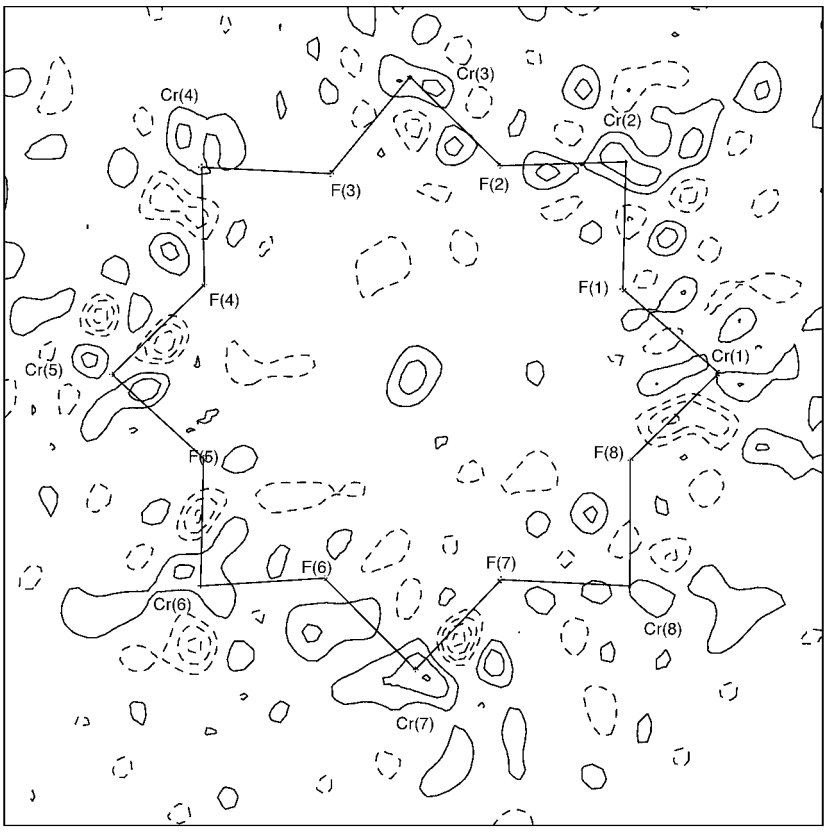

Figure 12. Residual density in the host molecular plane. Contours at 0.1 e Å^{-3}. Solid lines are positive contours, negative contours dashed. Zero contour omitted.

somewhat high $\Delta_{A\text{-}B}$ values for bonds involving the C atoms (C–C$^{\alpha}$: 19.8 pm^2; C–O: 14.3 pm^2; C$^{\alpha}$–C$^{\beta}$: 22.0 pm^2), but the values appear in general to be satisfactory. The refinement statistics for MM-II were almost as fine as for MM-I: $R_{II}(F^2) = 0.060$. Examination of the model density showed us that MM-II is preferable to MM-I, and thus MM-II was used in further analysis.

Compounds ***2*** *–* ***5***: All structures were solved by using direct methods.[32] Distance constraints were introduced to maintain the C–Me bond lengths in the pivalate groups at similar values. Hydrogen atoms were put at calculated ideal positions after each refinement cycle. All atoms (except for H) were refined anisotropically. The solvent molecules were located from difference Fourier maps. No distance constraints were introduced on these molecules, except for the CH_3CN and THF groups in **5**, which exhibited severe disorder. Several crystals of compound **5** from different syntheses were screened, and all showed tetragonal symmetry and good internal agreement of data. However, the refinements were all unexpectedly poor, and in some cases the structure could not be refined to an $R(F)$ value below 20%. Anisotropic refinement of methyl carbon atoms was not possible. In general, we observe that chromium wheel compounds crystallizing in this crystal system give diffraction data, which are difficult to model most likely due to the volatile disordered solvent molecules which sit between the Cr_8-molecules. When crystallized from tetrahydrofuran (THF) alone, the $[Cr_8F_8Piv_{16}]$ molecule crystallizes with disordered intermolecular THF in an orthorhombic spacegroup of dimensions $a = 18.822$, $b = 24.357$, $c = 32.274$ Å, $\alpha = \beta = \gamma = 90°$. The THF molecules are so poorly defined that we have chosen not to include this structure in Table 1. Besides the three monoclinic structures **2**–**4** the $[Cr_8F_8Piv_{16}]$ molecule is known to crystallize in the monoclinic spacegroup with acetone as a guest molecule[14] ($P2_1/c$, $a = 25.33$, $b = 16.68$, $c = 31.039$ Å, $\beta = 109.81°$).

CCDC-173968 (**1**), CCDC-173969 (**2**), CCDC-173970 (**3**), CCDC-173971 (**4**), and CCDC-173972 (**5**) contain the supplementary crystallographic data for this paper. These data can be obtained free of charge via www.ccdc.cam.ac.uk/conts/retrieving.html (or from the Cambridge Crystallographic Data Centre, 12 Union Road, Cambridge CB21EZ, UK; fax: (+44) 1223-336033; or deposit@ccdc.cam.uk).

Acknowledgements

The SUNY X3 beam line at the National Synchrotron Light Source (Brookhaven National Laboratory, USA) is supported by the Division of Basic Energy Sciences of the U.S. Department of Energy (DE-FG02-86ER45231). The synchrotron work is supported by a DANSYNC grant from the Danish Research Council. B.B.I. and S.P.P. are grateful to the Scientia Europaea Forum under the auspices of the French Academy of Science whose support made possible the initiation of the present study. We thank Professor John R. Eyler for suggestions to the manuscript.

[1] a) A. Villiers, *C. R. Hebd. Séances Acad. Sci.* **1891**, *112*, 435–437; b) A. Villiers, *C. R. Hebd. Séances Acad. Sci.* **1891**, *112*, 536–538.

[2] J. Szejtli, *Chem. Rev.* **1998**, *98*, 1743–1753.

[3] a) C. J. Pedersen, *J. Am. Chem. Soc.* **1967**, *89*, 2495–2496; b) C. J. Pedersen, *J. Am. Chem. Soc.* **1967**, *89*, 7017–7036.

[4] a) B. Dietrich, J.-M. Lehn, J. P. Sauvage, *Tet. Lett.* **1969**, *34*, 2885–2888; b) B. Dietrich, J.-M. Lehn, J. P. Sauvage, *Tet. Lett.* **1969**, *34*, 2889–2892; c) J.-M. Lehn, J. P. Sauvage, B. Dietrich, *J. Am. Chem. Soc.* **1970**, *92*, 2916–2918; d) J.-M. Lehn, *Acc. Chem. Res.* **1978**, *11*, 49–57; e) G. W. Gokel in *Monographs in supramolecular chemistry* (Ed.: J. F. Stoddart), The Royal Society of Chemistry, Cambridge, **1991**, p. 190.

[5] a) J. R. Moran, S. Karbach, D. J. Cram, *J. Am. Chem. Soc.* **1982**, *104*, 5826–5828; b) D. J. Cram, *Science* **1983**, *219*, 1177–1183.

[6] a) D. J. Cram, S. Karbach, Y. H. Kim, L. Baczynskyj, G. W. Kalleymeyn, *J. Am. Chem. Soc.* **1985**, *107*, 2575–2576; b) D. J. Cram, S. Karbach, Y. H. Kim, L. Baczynskyj, K. Marti, R. M. Sampson, G. W. Kalleymeyn, *J. Am. Chem. Soc.* **1988**, *110*, 2554–2560; c) L. M. Tunstad, J. A. Tucker, E. Dalcanale, J. Weiser, J. A. Bryant, J. C. Sherman, R. C. Helgeson, C. B. Knobler, D. J. Cram, *J. Org. Chem.* **1989**, *54*, 1305–1312.

[7] a) C. D. Gutsche, *Acc. Chem. Res.* **1983**, *16*, 161–170; b) C. D. Gutsche in *Monographs in supramolecular chemistry* (Ed.: J. F. Stoddart), The Royal Society of Chemistry, Cambridge, **1989**, p. 233; c) J. Vicens, V. Böhmer, *Calixarenes: A versatile class of macrocyclic compounds,* Kluwer, Dordrecht, **1991**. d) S. Shinkai, *Tetrahedron* **1993**, *49*, 8933–8968; e) V. Böhmer, *Angew. Chem.* **1995**, 107, 785; *Angew. Chem. Int. Ed. Engl.* **1995**, *34*, 713–745.

[8] a) D. J. Cram, J. M. Cram, *Acc. Chem. Res.* **1971**, *4*, 204–213; b) I. Tabushi, K. Yamamura, *Top. Curr. Chem.* **1983**, *113*, 145–182; c) Y. Murakami, *Top. Curr. Chem.* **1983**, *115*, 107–155; d) F. Diederich, *Angew. Chem.* **1988**, *100*, 372–396; Angew. *Chem. Int. Ed. Engl.* **1988**, *27*, 362–386; e) F. Diederich in *Monographs in supramolecular chemistry* (Ed.: J. F. Stoddart), The Royal Society of Chemistry, Cambridge, **1991**, p. 313.

[9] a) D. J. Cram, *Angew. Chem.* **1986**, 98, 1041–1060; *Angew. Chem. Int. Ed. Engl.* **1986**, *25*, 1039–1057; b) J.-M. Lehn, *Angew. Chem.* **1988**, *100*, 91–116; *Angew. Chem. Int. Ed. Engl.* **1988**, *27*, 89–112; c) D. J. Cram, *Science* **1988**, *240*, 760–767; d) D. J. Cram, *Angew. Chem.* **1988**, *100*, 1041–1052; *Angew. Chem. Int. Ed. Engl.* **1988**, *27*, 1009–1020; e) J.-M. Lehn, *Angew. Chem.* **1990**, *102*, 1347–1362; *Angew. Chem. Int. Ed. Engl.* **1990**, *29*, 1304–1319; f) D. J. Cram, *Nature* **1992**, *356*,

29 – 36; g) D. J. Cram, J. M. Cram in *Monographs in supramolecular chemistry* (Ed.: J. F. Stoddart), The Royal Society of Chemistry, Cambridge, **1994**, p. 223; h) J. W. Steed, J. L. Atwood, *Supramolecular chemistry*, Wiley, **2000**, p. 232.

[10] See special issue of *Chem. Rev.* **1998**, *98*, 1741 – 2076.

[11] The number of published papers on cyclodextrins alone is increasing exponentially, and the accumulated number of publications reached 10 000 some years ago.[2].

[12] A. Müller, H. Reuter, S. Dillinger, *Angew. Chem.* **1995**, *107*, 2505 – 2539; *Angew. Chem. Int. Ed. Engl.* **1995**, *34*, 2328 – 2361.

[13] M.-M. Rohmer, J. Devémy; R. Wiest, M. Bénard, *J. Am. Chem. Soc.* **1996**, *118*, 13 007 – 13 014.

[14] N. V. Gérbéléu, Yu. T. Struchkov, G. A. Timco, A. S. Batsanov, K. M. Indrichan, G. A. Popovich, *Dokl. Akad. Nauk. SSSR* **1990**, *313*, 1459 – 1462.

[15] J. van Slageren, R. Sessoli, D. Gatteschi, A. A. Smith, M. Helliwell, R. E. P. Winpenny, A. Cornia, A.-L. Barra, A. G. M. Jansen, E. Rentschler, G. A. Timco, *Chem. Eur. J.* **2002**, *8*, 277 – 285.

[16] a) M. Eshel, A. Bino, I. Felner, D. C. Johnston, M. Luban, L. L. Miller, *Inorg. Chem.* **2000**, *39*, 1376 – 1380; b) I. M. Atkinson, C. Benelli, M. Murrie, S. Parsons, R. W. P. Winpenny, *Chem. Commun.* **1999**, 285 – 286.

[17] *International Tables of Crystallography*, *Volume C*, **1992**, p. 700.

[18] A Cr–Cr distance of 2.818(2) Å has been observed in a Cr dimer, see: H. Toftlund, O. Simonsen, E. Pedersen, *Acta Chem. Scand.* **1990**, *44*, 676 – 682.

[19] a) Cr^{V}: C.-C. Wang, Y. Wang, L.-K. Chou, C.-M. Che, *J. Phys. Chem.* **1995**, *99*, 13 899 – 13 908; b) Cr^{II}: B. N. Figgis, C. J. Kepert, E. S. Kucharski, P. A. Reynolds, *Acta Crystallogr. Sect. B* **1992**, *48*, 753 – 761; c) C.-C. Wang, T.-H. Tang, Y. Wang, *J. Phys. Chem. A* **2000**, *104*, 9566 – 9572.

[20] C. Wilson, B. B. Iversen, J. Overgaard, F. K. Larsen, G. Wu, S. P. Palii, G. A. Timco, N. V. Gerbeleu, *J. Am. Chem. Soc.* **2000**, *122*, 11 370 – 11 379.

[21] R. F. W. Bader, *Atoms in Molecules: a quantum theory. International series of monographs on chemistry, Vol. 22*, Oxford University Press, Oxford, **1990**.

[22] a) Y. A. Abramov, *Acta Crystallogr. Sect. A* **1997**, *53*, 264 – 272. b) For a thorough presentation of these concepts in coordination compounds, see: P. Macchi, D. M. Proserpio, A. Sironi, *J. Am. Chem. Soc.* **1998**, *120*, 13 429 – 13 435.

[23] A. Holladay, P. Leung, P. Coppens, *Acta Crystallogr. Sect. A* **1983**, *39*, 377 – 387.

[24] B. Rees, A. Mitschler, *J. Am. Chem. Soc.* **1976**, *98*, 7918 – 7924.

[25] Z. W. Su, P. Coppens, *Acta Crystallogr. Sect. A* **1992**, *48*, 188 – 197.

[26] V. W. Day, W. G. Klemperer, O. M. Yaghi, *J. Am. Chem. Soc.* **1989**, *111*, 5959 – 5961.

[27] The electrospray ionization (ESI) mass spectra were recorded on a Bruker APEX 47e Fourier transform-ion cyclotron resonance (FT-ICR) mass spectrometer equipped with a modified (heated metal capillary) Analytica ESI source, and a 4.7 Tesla superconducting magnet. For analysis, the mother solution of sample **2** was diluted (1:10) with CH_2Cl_2 and infused at a rate of 1.25 μL min^{-1} using a Cole – Parmer single-syringe infusion pump. Charged droplets were produced by a 3.3 kV electrospray needle potential. Neither nebulizing gas nor drying gas was used. All aspects of pulse sequence control and data acquisition were performed using Bruker XMASS version 4.0 software running on a Silicon Graphics workstation.

[28] a) M. Vincenti, *J. Mass Spectrom.* **1995**, *30*, 925 – 939; b) M. Przybylski, M. O. Glocker, *Angew. Chem.* **1996**, *108*, 878 – 899; *Angew. Chem. Int. Ed. Engl.* **1996**, *35*, 807 – 826; c) E. Leize, A. Jaffrezic, A. VanDorsselaer, *J. Mass Spectrom.* **1996**, *31*, 537 – 544; d) J. A. Loo, *Mass Spectrom. Rev.* **1997**, *16*, 1 – 23; e) B. N. Pramanik, P. L. Bartner, U. A. Mirza, Y.-H. Liu, A. K. Ganguly, *J. Mass Spectrom.* **1998**, *33*, 911 – 920; f) H. Abdoul-Carime, *J. Chem. Soc. Faraday Trans.* **1998**, *94*, 2407 – 2410; g) C. A. Schalley, *Int. J. Mass Spectrom.* **2000**, *194*, 11 – 39; h) J. S. Brodbelt, *Int. J. Mass Spectrom.* **2000**, *200*, 57 – 69; i) J. B. Nicoll, D. V. Dearden, *Int. J. Mass Spectrom.* **2001**, *204*, 171 – 183; j) C. Collette, D. Dehareng, E. De Pauw, G. Dive, *J. Am. Soc. Mass Spectrom.* **2001**, *12*, 304 – 316; k) S. P. Palii, D. E. Richardson, M. L. Hansen, B. B. Iversen, F. K. Larsen, L. Sîngerean, G. A. Timco, N. V. Gerbeleu, K. R. Jennings, J. R. Eyler, *Inorg. Chim. Acta* **2001**, *319*, 23 – 42; l) D. P. Funeriu, K. Rissanen, J.-M. Lehn, *Proc. Natl. Acad. Sci. USA* **2001**, *98*, 10 546 – 10 551.

[29] a) K. Sannes-Lowery, R. H. Griffey, G. H. Kruppa, J. P. Speir, S. A. Hofstadler, *Rapid Commun. Mass Spectrom.* **1998**, *12*, 1957 – 1961; b) K. A. Sannes-Lowery, S. A. Hofstadler, *J. Am. Soc. Mass Spectrom.* **2000**, *11*, 1 – 9; c) K. Håkansson, J. Axelsson, M. Palmblad, P. Håkansson, *J. Am. Soc. Mass Spectrom.* **2000**, *11*, 210 – 217.

[30] a) The electron ionization (EI) mass spectra were recorded on a triple quadrupole Finnigan TSQ 7000 instrument. The analyzed compound was introduced in to the ion source of the mass spectrometer using a direct inlet probe. The temperature of the inlet system was 170 °C, ionizing electron energy 70 eV. b) Monoisotopic mass spectra were calculated from experimental mass spectra by using AELITA and ISOMETA programs: Yu. N. Sukharev, Yu. S. Nekrasov, N. S. Molgachova, E. E. Tepfer, *Org. Mass Spectrom.* **1991**, *26*, 770 – 776.

[31] L. Ribaud, G. Wu, Y. G. Zhang, P. Coppens, *J. Appl. Crystallogr.* **2001**, *34*, 76 – 79.

[32] SHELX-PC Package. Bruker Analytical X-ray Systems: Madison, WI, **1998**.

[33] R. H. Blessing, *J. Appl. Crystallogr.* **1997**, *30*, 421 – 426.

[34] T. Koritsanszky, S. T. Howard, T. Richter, P. R. Mallinson, Z. Su, N. K. Hansen, *XD. A Computer Program Package for Multipole Refinement and Analysis of Charge Densities from X-ray Diffraction Data*, Free University of Berlin, Berlin, **1995**.

[35] N. K. Hansen, P. Coppens, *Acta Crystallogr. Sect. A* **1978**, *34*, 909 – 921.

[36] E. Clementi, C. Roetti, *Atomic and Nuclear Data Tables* **1974**, *14*, 177 – 478.

[37] F. L. Hirshfeld, *Acta Crystallogr. Sect. A* **1976**, *32*, 239 – 244.

Received: November 19, 2001
Revised: February 28, 2002 [F3699]

  0947-6539/02/0812-2786 $ 17.50+.50/0